2018 European Control Conference (ECC)
June 12-15, 2018. Limassol, Cyprus

Gain-Scheduling Composite Nonlinear Feedback Control for a Set of 2nd Order Linear Parameter-Varying Systems*

Veli-Pekka Pyrhonen, *Student Member*, *IEEE*, Hannu J. Koivisto, and Matti K. Vilkko

***Abstract*— We present in this paper gain-scheduling composite nonlinear feedback (CNF) control for a set of second-order linear parameter-varying (LPV) systems that capture commonly used plant models in automatic control. The selected three parameter-varying plant models are double integrator with a gain, a series connection of an integrator and a first order system, and a second-order system without integration. We assume that the parameters of the plant models depend on an exogenous scheduling signal, which is unknown a priori, but it is measurable online and available for feedback control. The resulting model-based parameter-varying CNF controller assigns certain predefined properties for the closed-loop control system, which can be explained using linear time invariant (LTI) control theory. We demonstrate the proposed control structure with a simulation-based design example, in which a plant model is updated through a slowly varying scheduling signal, and, at the same time, the closed-loop system is commanded towards desired reference values. Our simulation results indicate that the closed-loop control system yields satisfactory tracking performance under parameter-varying conditions.**

I. Introduction

Composite nonlinear feedback (CNF) controllers consist of parallel-connected linear and nonlinear parts, which are separately designed such that closed-loop control system yields fast command following for a given reference input using constrained control. The design of a CNF controller can be done e.g., in terms of dynamic characteristics of initial and final closed-loop control systems: First, a lightly damped linear part is designed for swift response by placing the poles of the initial closed-loop system with small damping ratio. Then, the nonlinear part is designed such that the damping ratio of the closed-loop control system is gradually changed by smoothly relocating the poles of the initial system. The relocation mechanism can automatically be done as a function of control error, which improves the tracking performance of the closed-loop control system.

In this paper, we consider a set of second-order single input single output linear parameter-varying (SISOLPV) systems that capture dynamic characteristics of three commonly used plant models in automatic control; namely, 1) a double integrator with a gain, 2) a series connection of an integrator and a first-order system, and 3) a second-order system without integration. We allow all parameters of the SISOLPV plant models to vary according to a time-varying exogenous scheduling variable, or scheduling signal, say $\sigma(t)$. The trajectory of the scheduling signal is unknown a priori, but we assume that it is measurable online and available for feedback control.

Under the aforementioned conditions, we develop a model-based formulation for the CNF methodology such that closed-loop stability and some selected performance requirements can be satisfied for all σ. To achieve such objectives, we parameterize the CNF controller such that familiar results from the time invariant CNF are applicable to our parameter-varying case. We would like to note that there has been relatively little research as regards to gain-scheduling CNF control. We are only aware of our own application paper, which considers linearization-based gain-scheduling CNF control of a nonlinear chemical reactor [1].

In recent years, the CNF methodology has been found in variety of applications such as unmanned aerial vehicles [2–4], autonomous ground vehicles [5], underactuated surface vessels [6], hard disk drives [7], servo positioning systems [8–10], robot manipulators [11], and U-tube steam generators [12], to name a few.

II. Composite Nonlinear Feedback Control For a Set of 2nd Order LPV Systems

We consider in this paper the following SISOLPV plants with actuator nonlinearity

$$\begin{cases} \dot{x} = A(\sigma)x + B(\sigma)\mathrm{sat}(u) \\ y = C_y x \\ m = x \end{cases}, \; x(0) = x_0 , \qquad (1)$$

where $x \in \mathbb{R}^2$, $u \in \mathbb{R}$, $y \in \mathbb{R}$ and $m \in \mathbb{R}^2$ are the state, control input, controlled output and measured state, whereas x_0 is an initial condition. The symmetric actuator nonlinearity sat: $\mathbb{R} \rightarrow \mathbb{R}$ is given by

$$\mathrm{sat}(u) = \min\{u_{\max}, |u|\}\,\mathrm{sgn}(u) , \qquad (2)$$

where $u_{\max}$ is the saturation limit of the input and sgn denotes the sign function. We assume that the pair $(A(\sigma), B(\sigma))$ is completely controllable for all σ, and that the parameter-varying matrices $A(\sigma)$ and $B(\sigma)$ are of the form

$$A(\sigma) = \begin{bmatrix} 0 & 1 \\ a_{21}(\sigma) & a_{22}(\sigma) \end{bmatrix}, \; B(\sigma) = \begin{bmatrix} 0 \\ b(\sigma) \end{bmatrix}, \; b(\sigma) \neq 0 , \qquad (3)$$

where the elements $a_{21}(\sigma)$, $a_{22}(\sigma)$ and $b(\sigma)$ are analytic functions of σ. We note that $a_{21}(\sigma)$ and $a_{22}(\sigma)$ are allowed to be zero. Without any loss of generality, we assume that the output matrix C_y is

$$C_y = \begin{bmatrix} 1 & 0 \end{bmatrix} . \qquad (4)$$

*Research supported by Finnish Foundation for Technology.

V.-P. Pyrhonen, H. J. Koivisto and Matti K. Vilkko are with the Laboratory of Automation and Hydraulics, Tampere University of Technology, PL 692, 33101 Tampere, Finland (e-mail: veli-pekka.pyrhonen@tut.fi; hannu.koivisto@tut.fi; matti.vilkko@tut.fi).

Hence, the SISOLPV system (1) can be 1) a double integrator with a parameter-varying gain, 2) a series connection of an integrator and a parameter-varying first-order system, and 3) a parameter-varying second-order system without integration. We assume that σ is continuous and bounded function of t with bounded derivative, say $\dot{\sigma} \leq |\mu|$. We also assume that σ is known through measurements for all $t \geq 0$.

Here, our goal is to develop a model-based parameter-varying CNF control law for (1)–(4) such that the resulting closed-loop control system is stable and satisfy some design specifications for all σ. The design procedure is composed of two steps; namely, 1) the design of linear parameter-varying state feedback part, and 2) the design of parameter-varying nonlinear state feedback part. Finally, we connect the control laws from 1) and 2) in-parallel to form a parameter-varying gain-scheduled CNF control law.

Step 1. Design a linear parameter-varying full-state feedback control law

$$u_L = -K(\sigma)x + R_s(\sigma)r\,, \tag{5}$$

where r is the target step reference. The parameter-varying full-state feedback gain K is of the following form

$$\begin{aligned} K(\sigma) &= \begin{bmatrix} K_1(\sigma) & K_2(\sigma) \end{bmatrix} \\ &= \frac{1}{b(\sigma)}\begin{bmatrix} \omega_0^{\,2} + a_{21}(\sigma) & 2\xi_0\omega_0 + a_{22}(\sigma) \end{bmatrix}, \end{aligned} \tag{6}$$

where ξ_0 and ω_0 are called initial damping ratio and initial natural frequency. The gain K results in an initial closed-loop state matrix

$$A_{cl} = A(\sigma) - B(\sigma)K(\sigma) = \begin{bmatrix} 0 & 1 \\ -\omega_0^{\,2} & -2\xi_0\omega_0 \end{bmatrix},\ \forall \sigma\,, \tag{7}$$

which is Hurwitz and independent of σ. The parameters ξ_0 and ω_0 are chosen such that the step response of the initial closed-loop system has short rise time and large overshoot, i.e., $0 < \xi_0 < 1$ and $\omega_0 > 0$. The chosen state feedback gain also yields a parameter-varying reference tracking gain

$$R_s(\sigma) = -[C_y(A(\sigma) - B(\sigma)K(\sigma))^{-1}B(\sigma)]^{-1} = \omega_0^{\,2}\frac{1}{b(\sigma)}, \tag{8}$$

which assigns unity DC-gain for the closed-loop system from the target reference r to the controlled output y. Hence, the model-based closed-loop system is able to track constant references accurately in steady-state assuming disturbance free control environment and no modeling errors in (1).

Step 2. First, specify the desired state using

$$x_d \triangleq -A_{cl}^{-1}B(\sigma)R_s(\sigma)r = \begin{bmatrix} 1 & 0 \end{bmatrix}^T r\,. \tag{9}$$

Then form a CNF control law

$$u = u_L + u_N\,, \tag{10}$$

with a nonlinear parameter-varying feedback law u_N:

$$\begin{aligned} u_N &= \rho(r,y)B(\sigma)^T P(\sigma)\begin{bmatrix} x - x_d \end{bmatrix} \\ &= \rho(r,y)b(\sigma)\begin{bmatrix} p_{21}(\sigma) & p_{22}(\sigma) \end{bmatrix}\begin{bmatrix} x - x_d \end{bmatrix}, \end{aligned} \tag{11}$$

where the elements $p_{21}(\sigma)$ and $p_{22}(\sigma)$ need to be selected to yield a finite stable invariant zero for a certain auxiliary system, which is reviewed shortly. The function $\rho(r, y)$ is any nonpositive function, locally Lipschitz in y, that is used to smoothly change the closed-loop damping ratio when the output y of the system approaches the target step reference r. The resulting parameter-varying closed-loop state matrix is

$$\tilde{A}_{cl}(\sigma) = \begin{bmatrix} 0 & 1 \\ \tilde{a}_{21}(\sigma) & \tilde{a}_{22}(\sigma) \end{bmatrix} \tag{12}$$

with

$$\begin{cases} \tilde{a}_{21}(\sigma) = -\omega_0^{\,2} + \rho(r,y)b(\sigma)^2 p_{21}(\sigma) \\ \tilde{a}_{22}(\sigma) = -2\xi_0\omega_0 + \rho(r,y)b(\sigma)^2 p_{22}(\sigma) \end{cases}. \tag{13}$$

In what follows, we seek appropriate $p_{21}(\sigma)$ and $p_{22}(\sigma)$, which would make (12) independent of σ, and would yield a desired strictly real finite stable invariant zero for the auxiliary system. For such purpose, we need to revise the role of the auxiliary system that plays an important role within CNF framework. Please refer to Chen et al. [13] for more details as regards to fixed parameter systems.

Now, consider the block diagram in Fig. 1 with an auxiliary system Σ_{aux} and some function ρ as discussed above. In general, the auxiliary system in Fig. 1 can be written by

$$\begin{aligned} \Sigma_{aux}(\sigma) &= \begin{cases} \dot{x}_{aux} = A_{aux}(\sigma)x_{aux} + B_{aux}(\sigma)u_{aux} \\ y_{aux} = C_{aux}(\sigma)x_{aux} \end{cases} \\ \Rightarrow G_{aux}(s,\sigma) &= C_{aux}(\sigma)\left(sI - A_{aux}(\sigma)\right)^{-1}B_{aux}(\sigma)\,, \end{aligned} \tag{14}$$

where

$$\begin{cases} A_{aux}(\sigma) = A(\sigma) - B(\sigma)K(\sigma) \\ B_{aux}(\sigma) = B(\sigma) \\ C_{aux}(\sigma) = B(\sigma)^T P(\sigma) \end{cases}. \tag{15}$$

Given the SISOLPV system with (3) and the control law (5)–(6), the matrix collection in (15) becomes

$$\begin{cases} A_{aux}(\sigma) = A_{cl} \\ B_{aux}(\sigma) = \begin{bmatrix} 0 & b(\sigma) \end{bmatrix}^T \\ C_{aux}(\sigma) = b(\sigma)\begin{bmatrix} p_{21}(\sigma) & p_{22}(\sigma) \end{bmatrix} \end{cases}. \tag{16}$$

We know from the results of [13] that for time invariant fixed parameter systems, the auxiliary system G_{aux} is stable and minimum phase with relative degree equal to one.

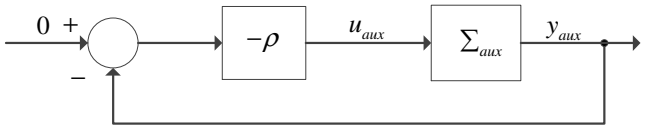

Figure 1. Closed-loop system with ρ and Σ_{aux}.

This fact motivates us to seek for the possibility of choosing $C_{aux}(\sigma)$ such that the results for fixed parameter systems apply to our parameter-varying case.

In our case, the system $G_{aux}(s, \sigma)$ in (14) is

$$G_{aux}(s,\sigma) = \frac{b^2(\sigma)\left(p_{22}(\sigma)s + p_{21}(\sigma)\right)}{s^2 + 2\xi_0\omega_0 s + \omega_0^2},\ \forall\sigma, \qquad (17)$$

where the elements $p_{21}(\sigma)$ and $p_{22}(\sigma)$ must be selected to yield a finite strictly real stable invariant zero, and a constant DC-gain for (17) for all σ. We therefore require that the output matrix $C_{aux}(\sigma)$ in (16) is of the following form

$$C_{aux}(\sigma) = b(\sigma)\left[\frac{\delta_1}{b(\sigma)^2} \quad \frac{\delta_2}{b(\sigma)^2}\right], \qquad (18)$$

for some real constants $\delta_1 > 0$ and $\delta_2 > 0$. We would like to note that the chosen $C_{aux}(\sigma)$ becomes parameter-varying gain of the nonlinear part in (11).

The output matrix in (18) results in the following G_{aux}

$$G_{aux}(s) = \frac{\delta_2 s + \delta_1}{s^2 + 2\xi_0\omega_0 s + \omega_0^2}, \qquad (19)$$

which is independent of σ, and which has a strictly real finite stable zero that can be placed precisely to $s = -\delta_1/\delta_2$. Therefore, one pole of the closed-loop system is drawn towards that invariant zero as $|\rho|$ increases, whereas the other pole approaches negative infinity as $|\rho| \to \infty$. Hence, suitable steady-state damping ratio and natural frequency for the final closed-loop control system can be achieved through an appropriate function ρ.

We are now ready to select an appropriate ρ to complete the CNF design. Research suggests several forms for the nonlinear function, see: [14–15]. We adopt in this paper the following scaled nonlinear function that was originally proposed by Lin in [16], and later revised by Lan in [14]:

$$\rho(r,y) = \rho(e) = -\beta\exp(-\alpha\alpha_0|e|),\ |e| = |r-y|, \qquad (20)$$

where

$$\alpha_0 = \begin{cases} \dfrac{1}{r-y_0}, & y_0 \neq r \\ 1, & y_0 = r \end{cases}. \qquad (21)$$

The function in (20)–(21) is able to adapt for varying step sizes, when CNF controller is commanded to follow non-unit step references. The tuning parameters $\alpha > 0$ and $\beta > 0$ are chosen such that the closed-loop system satisfies the desired transient performance requirements i.e., short settling time and small overshoot. It is simple to observe that

$$\lim_{t\to\infty}\rho(e) = -\beta, \qquad (22)$$

when $e \to 0$. Therefore, the parameter β can be selected to yield the desired damping ratio of the final system at the steady-state situation. Furthermore, the closed-loop characteristic equation of the final system i.e. when $\rho \to -\beta$, is given by

$$s^2 + \left(2\xi_0\omega_0 + \beta\delta_1\right)s + \left(\omega_0^2 + \beta\delta_2\right) = s^2 + 2\xi_\infty\omega_\infty s + \omega_\infty^2, \qquad (23)$$

where ξ_∞ is the damping ratio and ω_∞ is the natural frequency of the final system. Therefore, we can analytically solve the relation between ξ_∞ and β, which is

$$\xi_\infty = \frac{\xi_0\omega_0 + \frac{\beta}{2}\delta_1}{\sqrt{\omega_0^2 + \beta\delta_2}} = \frac{2\xi_0\omega_0 + \beta\delta_1}{2\sqrt{\omega_0^2 + \beta\delta_2}}. \qquad (24)$$

Using (24), we can e.g., specify the desired damping ratio of the final system and solve for β.

Finally, the parameter α needs to be selected to yield an appropriate convergence speed for ρ, when e becomes small. Usually, it is simple to find suitable value for α using few simulation tryouts. However, Lan et al. in [15] have proposed optimization approaches to automatically seek for an appropriate α by minimizing the well-known IAE (Integral of Absolute Error) or ITAE (Integral of Time multiplied by Absolute Error) criteria, which would deliver satisfactory performance. Nonetheless, the design of CNF controller is complete, when suitable α has been chosen. In what follows, we demonstrate the parameter-varying CNF control using a design example.

III. Design Example

Consider a moving ship with speed v and with heading angle θ. The heading angle θ can be altered by adjusting the rudder angle φ. A schematic diagram of the ship is depicted in Fig. 2. We adopt in this paper the following simplified model of the low-frequency motion of the ship [17]

$$\begin{aligned} &\tau(v(t))\cdot\ddot{\theta}(t) + \dot{\theta}(t) = k(v(t))\cdot\mathrm{sat}(\varphi(t)) \\ &\theta(0) = \theta_0,\ \varphi(0) = \varphi_0,\ \varphi \in [-60, 60], \end{aligned} \qquad (25)$$

where θ is the controlled output and φ is the control input, with θ_0 and φ_0 being the corresponding initial conditions. It should be noted that we have introduced an amplitude-constrained actuator into (25) to limit the control input and to make the original model more realistic.

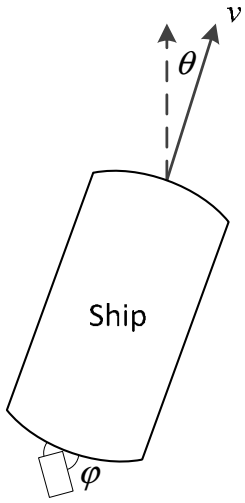

Figure 2. A moving ship with speed v and heading angle θ.

The parameters τ and k depend on the speed v according to the following expressions:

$$\tau(v(t)) = \tau_0 v_0 \frac{1}{v(t)} \tag{26}$$

and

$$k(v(t)) = \frac{k_0}{v_0} v(t)\,. \tag{27}$$

As expected, the turning dynamics is inversely proportional to speed v, whereas the gain k increases with increasing speed. We assign the following values for the constant parameters in (26) and (27): τ_0 = 10, v_0 = 10 and k_0 = 5, respectively. Furthermore, the speed $v(t)$ is the scheduling signal that is used to update the model. For conciseness, we omit the time dependence of the functions throughout the rest of the paper.

Automatic heading angle control is used in the speed range: $[v_{\min}, v_{\max}]$ = [1, 20], that is, the gain k varies in the range: $[k_{\min}, k_{\max}]$ = [0.5, 10], and τ in the range: $[\tau_{\min}, \tau_{\max}]$ = [5, 100]. Furthermore, we assume that the heading angle θ and speed v are measured and available for feedback control, whereas the rate of change of θ is constructed using the following first-order derivative filter

$$G(s) = \frac{s\omega_f}{s+\omega_f}\,, \tag{28}$$

where ω_f is the cut-off-frequency of the filter. In general, the cut-off frequency of the derivative filter is chosen such that appropriate filtering is maintained without distracting the signal components of the controlled output. Nonetheless, an LPV state-space representation of (25) is

$$\begin{bmatrix}\dot\theta\\ \ddot\theta\end{bmatrix} = \begin{bmatrix}0 & 1\\ 0 & -\tau(v)^{-1}\end{bmatrix}\begin{bmatrix}\theta\\ \dot\theta\end{bmatrix} + \begin{bmatrix}0\\ k(v)\tau(v)^{-1}\end{bmatrix}\text{sat}(\varphi)\,, \tag{29}$$

whereas the output equations are given by

$$y = \theta,\ m = \begin{bmatrix}\theta & \hat{\dot\theta}\end{bmatrix}^T,\ \hat{\dot\theta} = -\omega_f\hat\theta + \omega_f\theta,\ \hat\theta(0) = \hat\theta_0\,. \tag{30}$$

First, we illustrate the closed-loop performance for the frozen values of v = 1, 5, 10 and 20, respectively, and by using a single tuning linear full-state feedback law designed at the intermediate speed v = 10 only. The poles of the closed-loop system at this speed are placed at s = 1±j2. The unit step responses for the heading angle θ at each constant speed are depicted in Fig. 3.

Judging from the Fig. 3, a single tuning linear controller does not give satisfactory performance at the entire operation region. That is, the controller is experiencing severe difficulties when it is adjusting the rudder angle at low speeds owing to the small k and large τ. Hence, a need for more sophisticated control exists that can compensate for varying plant parameters, which, in this paper is, parameter-varying gain-scheduling. In what follows, we design a gain-scheduled parameter-varying CNF controller that is able to control the heading angle of the ship as desired despite the varying speed v.

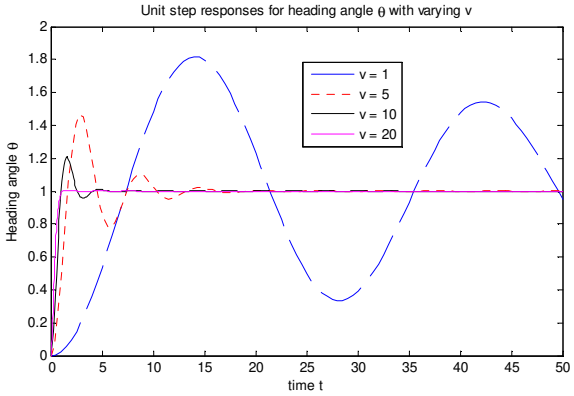

Figure 3. Heading angle responses for separate v.

First, we design a parameter-varying gain $K(v) = [K_1(v)\ K_2(v)] = [\omega_0^2 \quad (2\xi_0\omega_0 - \tau(v)^{-1})]\tau(v)/k(v)$ by placing the poles of the initial closed-loop system at s = –1±j2, which corresponds to $\xi_0 \approx 0.4472$ and $\omega_0 \approx 2.2361$. The parameter-varying reference tracking gain is then given by

$$R_s(v) = K_1(v) = -\frac{1}{b(v)}\omega_0^2 = -\frac{\tau(v)}{k(v)}\omega_0^2 = -\frac{\tau_0 v_0^2 \omega_0^2}{k_0}\frac{1}{v^2}\,. \tag{31}$$

Next, we choose δ_1 = 3.75 and δ_2 = 5.0, which place an invariant zero at s = –4/3 in the left half complex plane. We can therefore form the output matrix $C_{aux}(v)$ of the auxiliary system as

$$C_{aux}(v) = \frac{1}{b(v)}[\delta_1 \quad \delta_2] = \frac{\tau_0 v_0^2}{k_0}[\delta_1 \quad \delta_2]\frac{1}{v^2}\,. \tag{32}$$

Finally, we need to design the tuning parameters α and β of the nonlinear function (20) to achieve the desired closed-loop transient performance when e becomes small. That is, we need to specify the characteristics of the final system. Here, we aim to achieve a pair of strictly real poles at the negative real axis having damping ratio ξ_∞ = 1, which give $\beta \approx 2.5183$ according to (24). The resulting natural frequency of the final system is then given by $\omega_\infty \approx 17.5916$. The characteristics of the initial and final systems using root locus diagram is illustrated in Fig. 4.

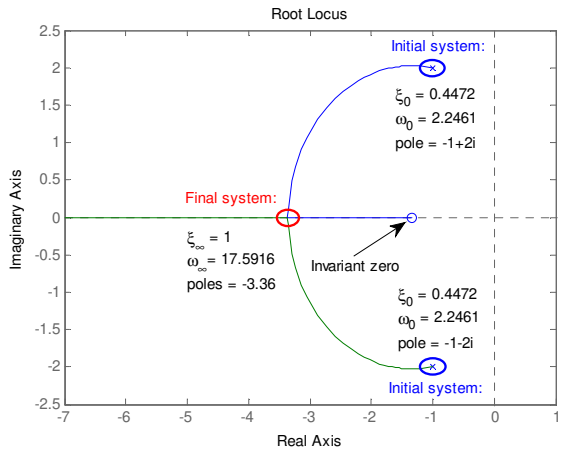

Figure 4. Root locus plot and pole-zero configurations of initial and final systems.

Thus, we now have a locus of closed-loop poles starting from the poles of the initial system that finally terminate at the negative real axis as specified by the final system. Such transition is smoothly and automatically delivered through ρ while $e \to 0$. To complete the CNF design, we need to find a suitable value for α, that is, we need to specify the convergence speed of ρ as e decreases.

We now seek an optimal value for the tuning parameter α by minimizing the IT^{2}AE-criterion [18]:

$$\min_{\alpha>0,\ \beta=2.5183} \int_0^\infty t^2 \left|\theta_r - \theta\right| dt\,, \tag{33}$$

where θ_r is the desired heading angle. The squaring of time in (33) assigns large penalty for errors occurring at the late stage of the transient response, and hence, we feel that (33) provides appropriate selectivity for our CNF design. We would like to note that minimizing ITAE yields small overshoot, because the resulting α is slightly too large. Nonetheless, IT^{2}AE performance index in a step experiment is uniquely minimized by α = 2.440, which completes the design of our CNF controller.

Finally, we collect the complete parameter varying CNF controller as

$$u = \varphi = -K(v)\begin{bmatrix}\theta\\ \dot{\hat{\theta}}\end{bmatrix} + R_s(v)\theta_r + \rho(e)B(v)^T P(v)\left(\begin{bmatrix}\theta\\ \dot{\hat{\theta}}\end{bmatrix} - \begin{bmatrix}1\\0\end{bmatrix}\theta_r\right)$$

$$= -\frac{\tau_0 v_0^{\,2}}{k_0}\frac{1}{v^2}\left[\omega_0^{\,2} \quad \left(2\xi_0\omega_0 - \frac{v}{\tau_0 v_0}\right)\right]\begin{bmatrix}\theta\\ \dot{\hat{\theta}}\end{bmatrix} + \left(-\frac{\tau_0 v_0^{\,2}\omega_0^{\,2}}{k_0}\frac{1}{v^2}\right)\theta_r$$

$$+\rho(e)\frac{\tau_0 v_0^{\,2}}{k_0}[\delta_2 \quad \delta_1]\frac{1}{v^2}\cdot\left(\begin{bmatrix}\theta\\ \dot{\hat{\theta}}\end{bmatrix} - \begin{bmatrix}1\\0\end{bmatrix}\theta_r\right),\ \dot{\hat{\theta}} = -\omega_f\hat{\theta} + \omega_f\theta,$$

$$\theta(0) = \theta_0,\ \hat{\theta}(0) = \hat{\theta}_0, \tag{34}$$

where

$$\rho(e) = -2.5183\exp(-2.440\alpha_0|e|),\ |e| = |\theta_r - \theta|\,, \tag{35}$$

$$\omega_f = 100, \tag{36}$$

$$\theta_0 = 0,\ \hat{\theta}_0 = 0,\ v(0) = 10,\ \varphi(0) = 0, \tag{37}$$

and where

$$\alpha_0 = \begin{cases}\dfrac{1}{\theta_r - \theta_0}, & \theta_0 \neq \theta\\ 1, & \theta_0 = \theta\end{cases}. \tag{38}$$

The schematic diagram of the closed-loop control system is depicted in Fig. 5. In what follows, we illustrate the closed-loop tracking performance using time-varying v. To make the simulation-based test more realistic, we continuously update the ship model using true v; however, the CNF controller is supplied with delayed and noise-corrupted v, as indicated in Fig. 5. We assume time delay d of 5 time units, and an additive zero-mean Gaussian white noise υ having a unit variance. Hence, the CNF controller is updated using $v_1 = v(t-d) + \upsilon$ rather than v.

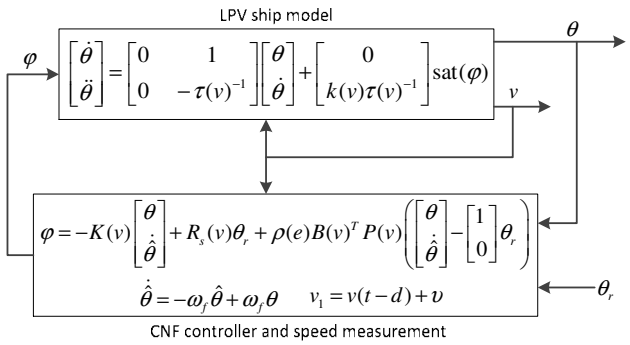

Figure 5. Closed-loop heading angle control.

Simulation test. The heading angle reference θ_r is a step sequence with changing step sizes. The speed v follows a time-varying profile in which acceleration, deceleration and constant speed occurs. The step sequence is configured such that the heading angle is changed while the ship is experiencing acceleration or deceleration. Hence, the turning dynamics of the ship change at the same time the heading angle is commanded towards different angle references.

The heading angle tracking performance, speed profiles, and rudder angle adjustments are depicted in Fig. 6. The erroneous speed profile v_1 is used to update the CNF controller, whereas the error-free profile v updates the ship model. That is, the CNF controller encounters considerable model mismatch during the test at several time instances. Nonetheless, the tracking performance is satisfactory despite the erroneous v_1 as can be seen from Fig. 6. We note that during the last two downward step changes, the rudder is turned much differently, despite the same step magnitude. Such behavior is rational, because the parameter-varying controller compensates for the slow speed of the ship i.e., for small k and large τ, which is most notable at t = 45. Also, small undershoot and overshoot are observed around t = 12 and t = 37, which results from the offset between v and v_1.

Furthermore, as $e \to 0$, the nonlinear part of the CNF controller is activated, and the poles of the closed-loop system is relocated as in Fig. 4, which mitigates the overshoot tendency caused by the lightly-damped initial system. Such feature is the key property of CNF control, which generally shortens the settling time of closed-loop control systems.

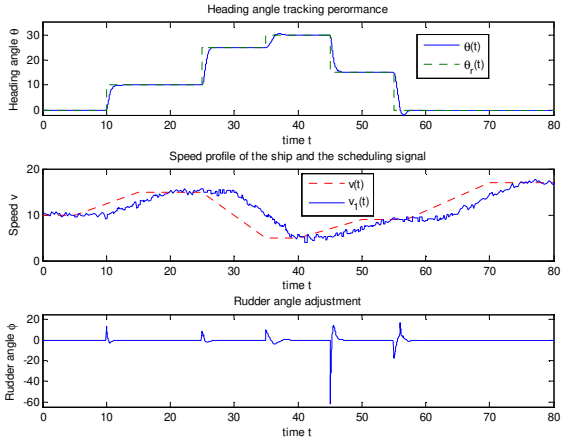

Figure 6. Heading angle, speed profiles, and rudder angle.

The gains of the time-varying nonlinear and linear parts are displayed in Fig. 7. We have simulated the gains in noise-free environment to make them more demonstrative. According to Fig. 7, the gains are appropriately updated towards large values when the speed of the ship is slow, and decreased when the ship advances faster in order to maintain the turning dynamics of the ship as desired.

Finally, we provide an estimate of the robustness properties of the control system for frozen values of the scheduling signal. In this case, the phase margin is a relevant measure, because the model-based gain margin is infinite. We can show that the worst-case phase margin for the CNF control is obtained at the initial stage i.e. when the nonlinear part is inactive. The worst-case phase margin in this case is 47.5 degrees, which is guaranteed at the entire operation region for all frozen values of v.

IV. Conclusion

In this paper, we presented gain-scheduling composite nonlinear feedback (CNF) control for a set of second-order linear parameter-varying (LPV) systems that capture commonly-used plant models in automatic control; namely, a double integrator with a parameter-varying gain, a series connection of an integrator and a parameter-varying first-order system, and a parameter-varying second-order system without integration. We demonstrated the proposed control structure with a simulation-based design example, in which a rudder angle of an LPV ship system was controlled in order to achieve desired heading angle under time-varying speed. Our simulation results indicated that the heading angle can satisfactorily be controlled despite intentional model mismatch introduced by inaccurate speed measurement, which functioned as the scheduling signal for the controller. We feel that our study may lay foundation for generalizing CNF control for more general class of LPV systems that were not considered in this paper.

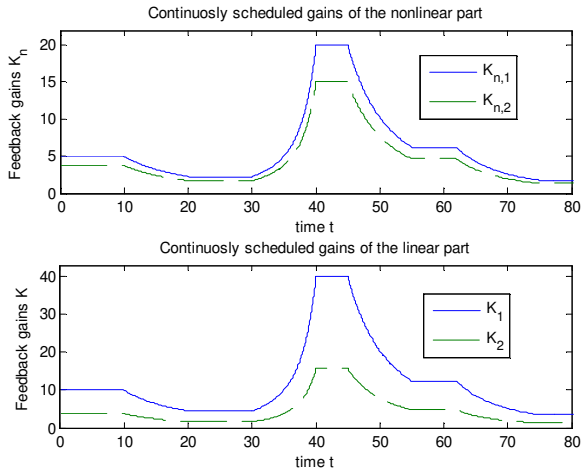

Figure 7. Controller gains as a function of time.

References

[1] V.-P. Pyrhonen, and H. J. Koivisto, "Gain-scheduled composite nonlinear feedback control of an exothermic chemical reactor," in *Proc. 15th European Control Conf.*, Aalborg, Denmark, June–July 2016, pp. 67–73.

[2] Z. Hou and I. Fantoni, "Interactive leader-follower consensus of multiple quadrotors based on composite nonlinear feedback control," *IEEE Trans. Contr. Syst. Technol.*, vol. PP, pp. 1–12, Oct. 2017.

[3] G. Cai, B.M. Chen, K. Peng, and M. Dong, "Modeling and control of the yaw channel of a UAV helicopter," *IEEE Trans. Ind. Electron.*, vol. 5, pp. 3426–3434, Sep. 2008.

[4] K. Li, K. Wang, K. Zhang, and B.M. Chen, "Aggressive maneuvers of a quadrotor MAV based on composite nonlinear feedback control," in *Proc. 2016 IEEE International Conf. on Advanced Intelligent Mechatronics (AIM)*, Banff, Alberta, Canada, July 2016, pp. 513–518.

[5] C. Hu, R. Wang, F. Yan, and H.R. Karimi, "Robust composite nonlinear feedback path-following control for independently actuated autonomous vehicles with differential steering," *IEEE Trans. Tranport. Electrific.*, vol. 2, pp. 312–321, Mar. 2016.

[6] C. Hu, R. Wang, F. Yan, and N. Chen, "Robust composite nonlinear feedback path-following control for underactuated surface vessels with desired-heading amendment," *IEEE Trans. Ind. Electron.,* vol. 63, pp. 6386–6394, May 2016.

[7] W. Lan, C.K. Thum, and B.M. Chen, "A hard disk drive servo system design using composite nonlinear feedback control with optimal nonlinear gain tuning methods," *IEEE Trans. on Ind. Electron.*, vol. 57, pp. 1735–1745, Sep. 2010.

[8] G. Cheng, and K. Peng, "Robust composite nonlinear feedback control with application to a servo positioning system," *IEEE Trans. Ind. Electron.*, vol. 54, pp.1132–1140, Apr. 2007.

[9] G. Cheng, and J–G. Hu, " An observer-based mode switching control scheme for improved position regulation in servomotors," *IEEE Trans. Contr. Syst. Technol.*, vol. 22, pp. 1883–1891, Dec. 2013.

[10] V.-P Pyrhonen, H.J. Koivisto and M.K. Vilkko, "A reduced-order two-degree-of-freedom composite nonlinear feedback control for a rotary DC servo motor," in *Proc. 56th IEEE Conf. on Decision and Control,* Melbourne, Australia, Dec. 2017, pp. 2065–2071.

[11] P. Wendong, and S. Jianbo, "Tracking controller for robot manipulators via composite nonlinear feedback law," *IEEE J. Syst. Eng. Electron.*, vol. 20, pp. 129–135, Jan 2012.

[12] L. Wei, F. Fang, and Y. Shi, "Adaptive backstepping-based composite nonlinear feedback water level control for the nuclear u-tube steam generator," *IEEE Trans. Contr. Syst. Technol.*, vol. 22, pp. 369–377, Mar. 2013.

[13] B.M. Chen, T.H. Lee, K. Peng, and V. Venkataramanan, "Composite nonlinear feedback control for linear systems with input saturation: theory and an application," *IEEE Trans. Autom. Contr.*, vol. 48, pp. 427–439, Mar. 2003.

[14] W. Lan, and B.M. Chen, "On selection of nonlinear gain in composite nonlinear feedback control for a class of linear systems," in *Proc. 46th IEEE Conf. on Decision and Control*, New Orleans, LA, USA, Dec. 2007, pp. 1198–1203.

[15] W. Lan, C.K. Thum, and B.M. Chen, "A hard disk drive servo system design using composite nonlinear feedback control with optimal nonlinear gain tuning methods," *IEEE Trans. on Ind. Electron.*, vol. 57, pp. 1735–1745, Sep. 2010.

[16] Z. Lin, M. Pachter, and S. Banda, "Toward improvement of tracking performance – nonlinear feedback for linear systems," *Int. J. Contr.*, vol. 70, pp. 1–11, Nov. 1998.

[17] H. K. Khalil, *Nonlinear Systems*, 3rd ed., Prentice Hall, Upper Saddle River, New Jersey, 2002, p. 501.

[18] K.J. Astrom, and T. Hagglund, *Advanced PID Control*, ISA – Instrumentation, Systems, and Automation Society, Research Triangle Park, North Carolina, 2006, pp. 105–113.